A Combined Electronic Position- and Partial Amplitude-Control Synthesis Technique for Sidelobe Reductions in Linear Array Antennas

Maria Pour, *Senior Member, IEEE*, Tanzeela H. Mitha, *Member, IEEE*, and Eli C. Brothers, *Student Member, IEEE*

***Abstract*— An electronic-position synthesis technique in conjunction with a partial amplitude-control synthesis technique is employed in small-scale, equally spaced linear arrays to reduce the side and minor lobe levels. The electronic-position synthesis technique is made possible through the use of dual-mode antenna elements, capable of electronically displacing their phase center locations, and thus changing their relative coordinates within the array configuration. This will result in electronically breaking the periodicity of the array, and when combined with the amplitude-tapered side elements, it will facilitate an unprecedented sidelobe reduction that is on par with the conventional amplitude-control only such as Chebyshev. In the proposed method, only the amplitude coefficients of selected side elements need to be tapered using stepped functions. For the proof of concept, three different case studies, consisting of 7-, 9-, and 11-element linear arrays, will be investigated. To further validate the results in practice, the nine-element antenna array is fabricated and tested, whose full-wave simulated and measured results are in good agreement.**

***Index Terms*— Amplitude-control, electronic position-control, phased array antennas, sidelobe levels (SLLs).**

I. Introduction

PHASED array antennas have been instrumental in advancing state-of-the-art technologies in a variety of applications ranging from remote sensing, navigation, biomedical imaging, and smart cities to homeland security systems, due to their appealing capabilities of realizing unique radiation characteristics such as beam scanning, sidelobe level (SLL) control, and many more [1]. Different synthesis techniques, mainly based on amplitude-, phase-, and position control, or a combination of these, have been reported in the literature. For instance, the SLLs can be primarily controlled using the amplitude-control synthesis technique such as Binomial [2], Dolph-Chebyshev [3], and Taylor methods [4], [5] in equally spaced array antennas. The SLLs can also be controlled by the phase-only synthesis technique [6], [7], [8] and the combined phase- and amplitude-synthesis technique [9], [10], [11], [12], [13], [14], [15], [16]. However, they do require specific phase shifters, which will restrict the main beam scanning capability of phased array antennas. Harrington [17] proposed the position-control synthesis technique in uniformly excited array antennas by physically changing the interelement spacing, which was further investigated in [19], [20], [21], [22], [23], [24], [25], [26], [27], and [28]. A vast variety of evolutionary algorithms, such as genetic algorithm (GA), particle swarm optimization (PSO), and differential evolution (DE), were developed to optimize the element positions and excitation coefficients [29], [30], [31], [32], [33], [34], [35], [36], [37], [38], [39], [40], [41], [42], [43], mainly for SLL reduction purposes. However, for a given criterion, it was required either to turn off different elements in large arrays or physically move the base elements of the array to predetermined positions, making the overall system rigid and expensive in practice. To mitigate this, a novel technique of electronically changing the relative coordinate of each element by displacing the phase center locations of dual-mode antenna elements [44] in linear array antennas was proposed by the authors in [45] and [46] to modify the radiation pattern without any physical displacement. When combined with the array thinning in large linear array antennas, it was shown that one could achieve SLLs as low as −21 dB. However, in small linear array antennas, about 4–5 dB SLL reduction is achievable using the electronic position-control synthesis technique only and array thinning is not quite feasible.

Herein, to further suppress the side and minor lobe levels, the electronic-position control synthesis technique is combined with the partial amplitude-control method such that the amplitude distribution of the side elements only is tapered to form a symmetric stepped function. The preliminary analytical results for a seven-element linear array [47] were recently presented at the 2022 IEEE International Symposium on Phased Array Systems and Technology. Herein, the proposed concept is further explored in 9- and 11-element equally spaced, linear array antennas with different percentages of tapered side elements to realize unprecedented SLL reductions that are comparable to conventional Chebyshev distributions. To further validate the

Manuscript received 17 March 2023; revised 30 May 2023; accepted 7 June 2023. This work was supported in part by the National Science Foundation (NSF) the Faculty Early Career Development (CAREER) under Award ECCS-1653915; and in part by the Alabama EPSCoR Graduate Research Scholars Program (GRSP), Rounds 15, 16, and 17. This article is an extended version from the 2022 IEEE International Symposium on Phased Array Systems and Technology, Waltham, MA, USA, 11–14 October 2022. *(Corresponding author: Maria Pour.)*

The authors are with the Department of Electrical and Computer Engineering, The University of Alabama in Huntsville, Huntsville, AL 35899 USA (e-mail: maria.pour@uah.edu).

Color versions of one or more figures in this article are available at https://doi.org/10.1109/TMTT.2023.3288634.

Digital Object Identifier 10.1109/TMTT.2023.3288634

results of the proposed method in practice, the nine-element array was fabricated and successfully tested.

II. Electronic Position Control Technique and Array Formulation

The underlying principle of the electronic position control technique is established by the authors in [45] and herein it is briefly reviewed. It is known that the phase center location of a single-mode circular patch antenna is coincident with its physical center. Interestingly, when two or multiple modes are simultaneously excited with proper phase shifts, its effective phase center can be displaced from its physical center. When this intriguing property is utilized in an array context, the relative coordinates of its base elements can be electronically changed, which is the basis of the electronic position control technique. To make the constituent elements of the arrays as compact as possible, the first two transverse magnetic (TM) modes of circular microstrip patch antennas are employed, namely, the TM_{11} and TM_{21} modes. The θ-component of the radiation function of an x-polarized TM_{11} mode is governed by

$$f_{11} = -j[J_o(a_1 u) - J_2(a_1 u)]\cos\phi \tag{1}$$

where $u = k_o \sin\theta$, k_o is the wavenumber, a_1 is the radius of the TM_{11} patch, and J_n is the Bessel function of the first kind and order n. As for the x-polarized TM_{21} mode, the θ-component of its radiation function is expressed by

$$f_{21} = [J_1(a_2 u) - J_3(a_2 u)]\cos 2\phi \tag{2}$$

where a_2 is the radius of the TM_{21} patch. Combining these two modes yields the following element pattern, electronically facilitating the phase center displacement away from the physical center of the patch

$$f = -j\{[J_o(a_1 u) - J_2(a_1 u)]\cos\phi + jA_{21}[J_1(a_2 u) - J_3(a_2 u)]\cos 2\phi\} \tag{3}$$

where A_{21} is a complex number describing the magnitude and phase relationship between the two modes, called the mode content factor. As described in [44], [45], and [46], this mode content factor can be used to control the displacement of the phase center of the sum of the two modes. This is done by selecting the ratio of magnitudes $|A_{21}|$ and the phase difference between the modes α_{21}, which are components of the mode content factor given by

$$A_{21} = |A_{21}|\angle a_{21}. \tag{4}$$

These dual-mode antennas, called electronically displaced phase center antennas (E-DPCA), can be used as the basis for a linear array in which their relative coordinates within the array configuration can be electronically changed by displacing their phase centers along the axis of the array. A diagram of the general case of this array is depicted in Fig. 1, where the phase center of each element is shown as an "eye" displaced from the element's physical center. These "eyes" are displaced to form a symmetrical, electronically aperiodic array, with the blue "eyes" and green "eyes" representing in- and out-of-phase excitations, respectively, of the two modes. The E-DPCA technique is equally applicable to odd and even numbers of elements. In this article, without the loss of generality, odd-numbered arrays with the number of elements of $N = 2M + 1$ are studied.

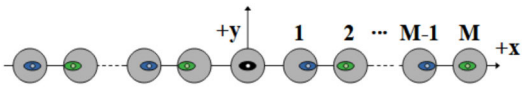

Fig. 1. Structure of the $(2M+1)$-element E-DPCA array whose elements are physically placed $0.7\lambda_o$; the phase center locations are marked with colored eye symbols in black, blue, and green, respectively, indicating that the phase center is moved to the center, right, and left of the base element.

Based on the array multiplication rule [1], the total radiation pattern of the array is equal to the product of the element pattern and the array factor, which will be presented throughout this article. Therefore, for the $(2M + 1)$-element EDPA array, shown in Fig. 1, assuming that the array has right-left symmetry in terms of the electronic position of its base elements, as well as the magnitude excitation coefficients, denoted by C_m, the θ-component of the array radiation function can be expressed by

$$F = C_0 f_{11} + 2\sum_{m=1}^{M} C_m\left[f_{11}\cos(mX) + jA_{21}(m) f_{21}\sin(mX)\right] \tag{5}$$

where $X = kd\sin\theta\cos\phi$, taking into account the phase delay caused by the element placement along the x-axis with reference to the coordinate origin, and d is the physical spacing between the elements. To avoid having grating lobes and keep the mutual coupling between the elements below the -10 dB level, the element spacing is selected as $0.7\lambda_o$, where λ_o is the free-space wavelength at 10 GHz.

The built-in GA in MATLAB is used to determine the optimal mode content factors and amplitude weighting of these linear arrays. To keep the broadside shape of the element patterns, the upper limit of the magnitude of the mode content factors was set to unity. The phase shift of either 0° or 180° is applied between the modes to maximize the phase center displacement of the elements. To progress toward the optimal values, the following fitness function is defined such that the first null beamwidth (FNBW) of the E-DPCA plus partial amplitude tapered array is as close as possible to that of its counterpart Chebyshev array for a given desired SLL

$$\mathrm{FF_{GA}} = 10(|\mathrm{SLL} - \mathrm{SLL_{Cheb}}|) + (e^{|\mathrm{FNBW} - \mathrm{FNBW_{Cheb}}|} - 1) \tag{6}$$

where $\mathrm{SLL_{Cheb}}$ and $\mathrm{FNBW_{Cheb}}$ are the SLL and FNBW of the counterpart Chebyshev array consisting of conventional single-mode elements, respectively.

III. Analytical Results of Linear Arrays

A. Seven-Element Array

In addition to the electronic position control from the E-DPCA method, further side and minor lobe suppression can be achieved by applying amplitude tapers to the edge elements

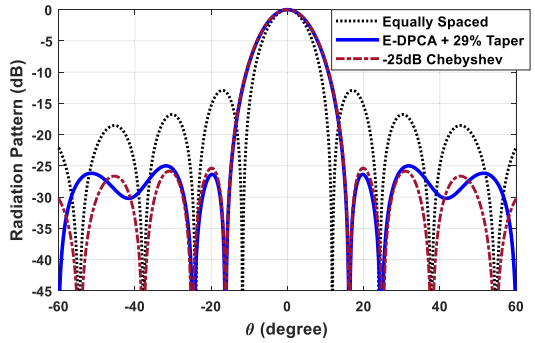

Fig. 2. Normalized radiation patterns of the equally spaced uniform and conventional −25 dB Chebyshev of single-mode elements, as well as the E-DPCA seven-element linear arrays with $M = 3$ in Fig. 1.

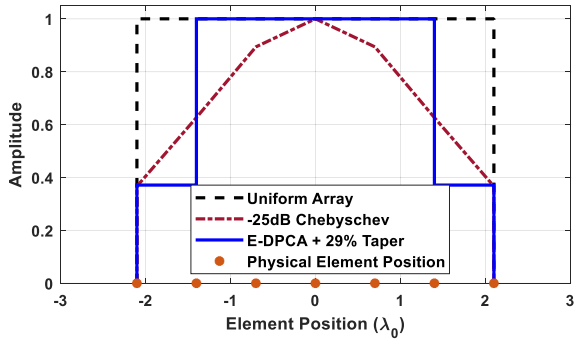

Fig. 3. Comparison of amplitude coefficients for the uniform, −25 dB Chebyshev, and E-DPCA with 29% edge taper case in the seven-element array.

of the array. In the seven-element array, we consider the case in which the two edge elements, one on each side, are engaged, which is 29% of the elements in the array. By tapering these elements, an SLL of −25 dB can be obtained, which is an improvement of 12 dB over the uniformly excited array. It should be noted that with the E-DPCA technique alone in such a small array only about 5 dB SLL reduction would be achieved, as reported in [46]. As opposed to conventional Chebyshev arrays, which require heavily tapered amplitude coefficients applied to all elements, in the proposed concept, only a fraction of the elements are tapered while the results are quite comparable to the traditional SLL synthesis technique without further broadening the FNBWs or compromising the directivity. This signifies the advantage of the proposed partial amplitude, electronic-position control method. The normalized radiation pattern given by the partial amplitude-controlled E-DPCA method is displayed in Fig. 2 and compared to the −25 dB Chebyshev array as well as the uniformly excited, equally spaced array.

The amplitude excitations for the partial amplitude-controlled array are shown in Fig. 3 in comparison to the uniformly excited case and a standard −25 dB Chebyshev distribution. It is worth noting that the −25 dB SLL is achieved without having to use the heavily tapered coefficients of the −25 dB Chebyshev array counterpart.

The mode content factors are enumerated in Table I. Since in these cases, we limit α_{21} to either 0° or 180°, we list a real-valued A_{21} in which a negative value indicates a shift of the phase center in the $-x$ direction and a positive value indicates a shift in the $+x$ direction.

TABLE I
MODE CONTENT FACTORS FOR THE SEVEN-ELEMENT ARRAY

Element	A_{21}
1	-0.91
2	-0.13
3	0.89

TABLE II
MODE CONTENT FACTORS FOR THE NINE-ELEMENT ARRAYS

Element	A_{21} for 22% tapered	A_{21} for 44% tapered	A_{21} for 67% tapered
1	-0.63	-0.66	-0.72
2	-0.86	-0.49	-0.62
3	-0.49	0.26	0.09
4	0.97	0.56	0.41

Based on the results plotted in Fig. 2, it is clear that with the reduced SLL, the FNBW of the proposed array increases compared to the uniformly excited, equally spaced array leading to the directivity drop which inevitably occurs in array antennas with reduced SLLs. The extreme case would be that of the binomial array producing the broadest main beam with no sidelobes when the element spacing is equal to or less than half a wavelength [1]. Interestingly, the beam broadening factor of the proposed array is on par with the −25 dB Chebyshev array counterpart. Further details on the peak directivity, SLLs, and FNBWs of these arrays will be provided for different case studies at the end of Section III.

B. Nine-Element Array

The next set of cases is those of a nine-element array with $0.7\lambda_o$ spacing. We again consider the case in which two elements (22%) are engaged with amplitude tapering to achieve an SLL of −20 dB. Additionally, having more elements in the array, further partial amplitude tapering is carried out through the cases of four edge elements (44%) and six edge elements (67%) leading to the realization of −25 and −30 dB of SLLs, respectively. The corresponding total radiation patterns are plotted in Fig. 4 and compared to their uniform and Chebyshev array counterparts consisting of single-mode elements. The amplitude excitations for the nine-element array cases are shown in Fig. 5. The corresponding mode content factors are listed in Table II. Their radiation characteristics will be further addressed.

C. Eleven-Element

Finally, the set of 11-element array cases is considered with the same $0.7\lambda_o$ spacing. Using two engaged edge elements (18%), we can again achieve an SLL of −20 dB. Engaging four edge elements (36%) yields an SLL of −25 dB, and six edge elements (54%) give −30 dB of SLL; all of these results are plotted in Fig. 6 and compared to the uniform, equally spaced, and their counterpart Chebyshev arrays. As observed, the proposed array enables the same SLL reductions as its equivalent Chebyshev, without having to heavily taper the

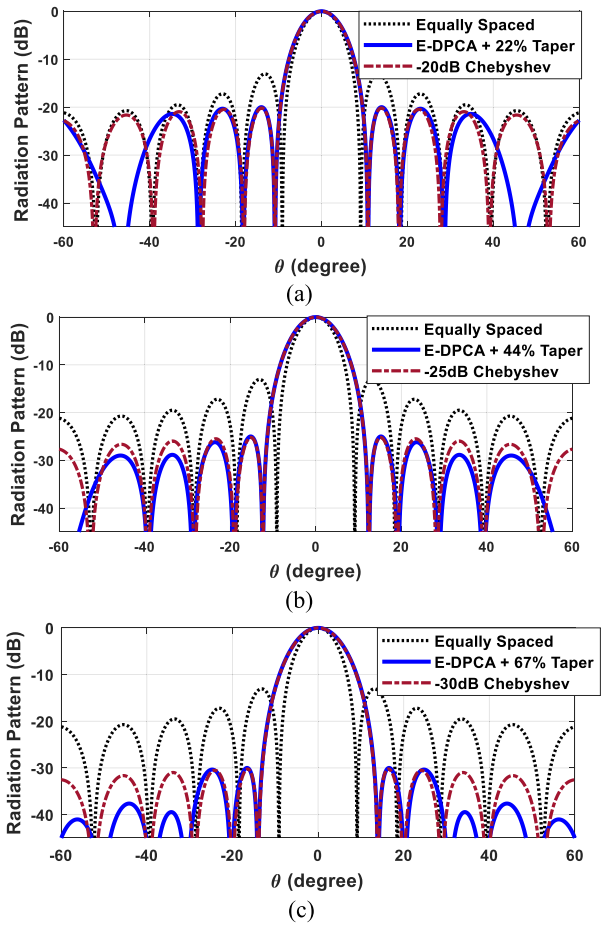

Fig. 4. Normalized radiation patterns of the nine-element linear arrays for the equally spaced uniform and conventional −30 dB Chebyshev of single-mode elements, as well as the E-DPCA arrays with (a) two edge elements, (b) four edge elements, and (c) six edge elements tapered.

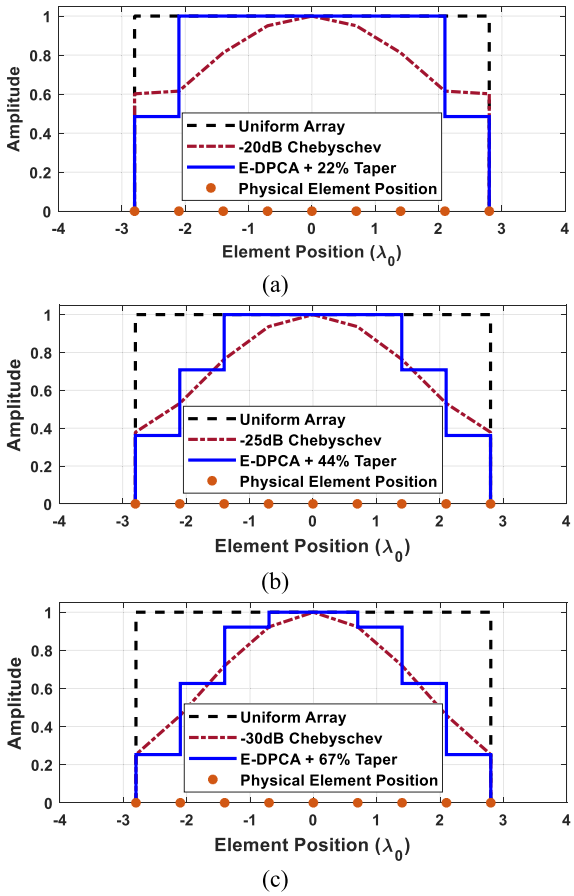

Fig. 5. Amplitude coefficients for the uniform, Chebyshev, and E-DPCA with edge taper cases in the nine-element array for (a) two edge elements, (b) four edge elements, and (c) six edge elements tapered.

TABLE III

MODE CONTENT FACTORS FOR THE 11-ELEMENT ARRAYS

Element	A_{21} for 18% tapered	A_{21} for 36% tapered	A_{21} for 54% tapered
1	-1.00	-0.92	-0.42
2	-1.00	-0.86	-0.13
3	0.99	-0.15	-0.52
4	0.68	0.74	0.66
5	1.00	0.63	0.33

amplitude distribution of all the elements. For further clarification, the amplitude distributions for the aforementioned 11-element array cases are overlaid in Fig. 7. For the proposed E-DPCA plus partial amplitude control method, the corresponding mode content factors are listed in Table III for different percentiles of tapered elements.

It is instructive to further investigate the radiation characteristics of the presented linear arrays with different cases in terms of peak directivity, SLL, and FNBW. These are all listed in Table IV for the 7-, 9-, and 11-element arrays, comparing their performances in equally spaced, E-DPCA only, counterpart Chebyshev, and the proposed E-DPCA plus partially amplitude tapered arrays. As observed, the directivity and FNBWs of the proposed E-DPCA plus partially amplitude tapered array are almost the same as its respective Chebyshev array, while a substantial SLL reduction is made possible using the proposed technique by amplitude tapering a lesser fraction of the elements.

TABLE IV

COMPARISON OF DIRECTIVITY, SLL, AND FNBWS OF THE 7-, 9-, AND 11-ELEMENT ARRAYS WITH DIFFERENT CASE STUDIES

Arrays		Directivity (dBi)	SLL (dB)	FNBW
7-element	Equally-Spaced	16.6	-13	24.4°
	E-DPCA only	16.2	-17.7	24.4°
	E-DPCA + 29% tapered	16.0	-25	32°
	-25dB Chebyshev	16.1	-25	32°
9-element	Equally-Spaced	17.6	-13	18°
	E-DPCA only	16.8	-17.8	18°
	E-DPCA + 67% tapered	16.3	-30	27.2°
	-30dB Chebyshev	16.4	-30	27.2°
11-element	Equally-Spaced	18.9	-13	15°
	E-DPCA only	16.8	-17.8	15°
	E-DPCA + 54% tapered	17	-30.1	23°
	-30dB Chebyshev	17.4	-30	22.4°

IV. MEASURED RESULTS

To validate the results, the fabricated nine-element array in [46] was utilized, consisting of concentric circular and annular ring patches [48], exciting the TM_{11} and TM_{21}

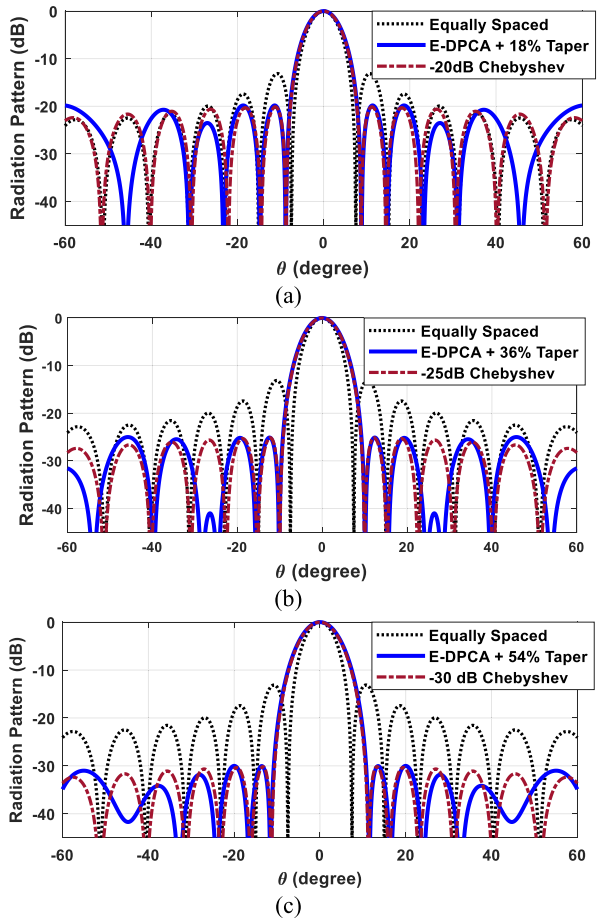

Fig. 6. Normalized radiation patterns of the 11-element linear arrays for the equally spaced uniform and Chebyshev of single-mode elements, as well as the E-DPCA with (a) two edge elements, (b) four edge elements, and (c) six edge elements tapered.

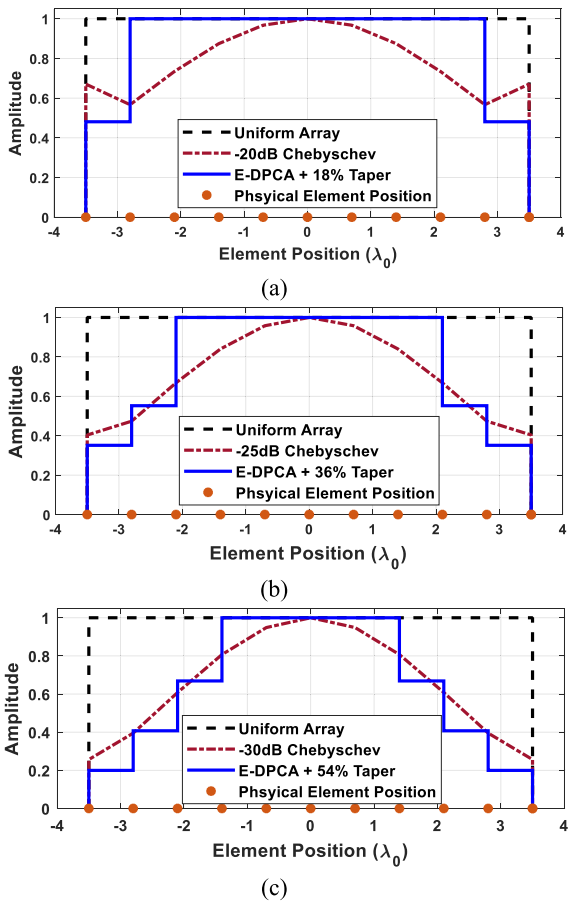

Fig. 7. Amplitude coefficients for the uniform, Chebyshev, and E-DPCA with edge taper cases in the 11-element array for (a) two edge elements, (b) four edge elements, and (c) six edge elements tapered.

TABLE V

COMPARISON WITH PHASE-ONLY SIDELOBE SUPPRESSION TECHNIQUE [7]

Method Used	Number of Elements	Linear Array Length in λ_0	Maximum SLL in dB
Phase-only [7]	20	9.5	-15.8
	80	39.5	-20.1
	500	249.5	-25.4
The proposed combined electronic position- and partial amplitude control technique	7	4.2	-25
	9	5.6	-30

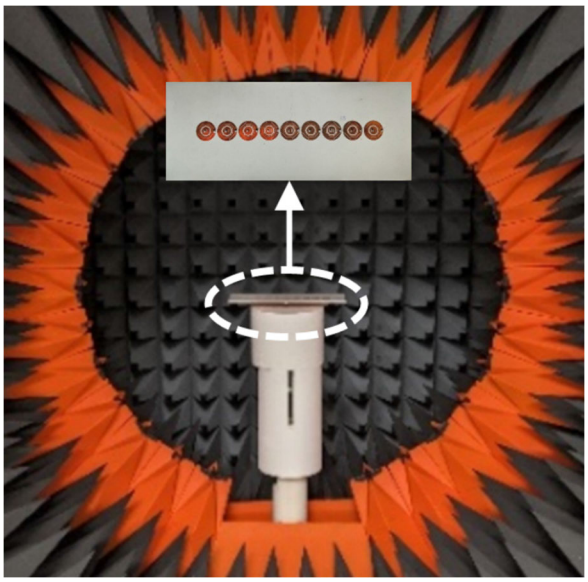

Fig. 8. Nine-element linear E-DPCA array prototype under test in UAH's near-field anechoic chamber.

modes, respectively, designed at 10 GHz. The TM_{11} mode is excited in the central disk patch with a radius of 4.16 mm, while the TM_{21} mode is produced in the concentric ring with inner and outer radii of 4.9 and 9.751 mm, respectively. The detailed description of the array structure and the elements is provided in [46] and thus is omitted here for brevity. The array prototype was measured in the spherical near-field anechoic chamber at the University of Alabama in Huntsville (UAH) as seen in Fig. 8.

The array radiation patterns were computed using the well-established "active element pattern" technique described in [49] and [50]. Based on this technique, the active radiation patterns of the center and edge elements of the nine-element array were measured while terminating all other elements with 50 Ω loads. As such, for the proposed dual-mode array, the

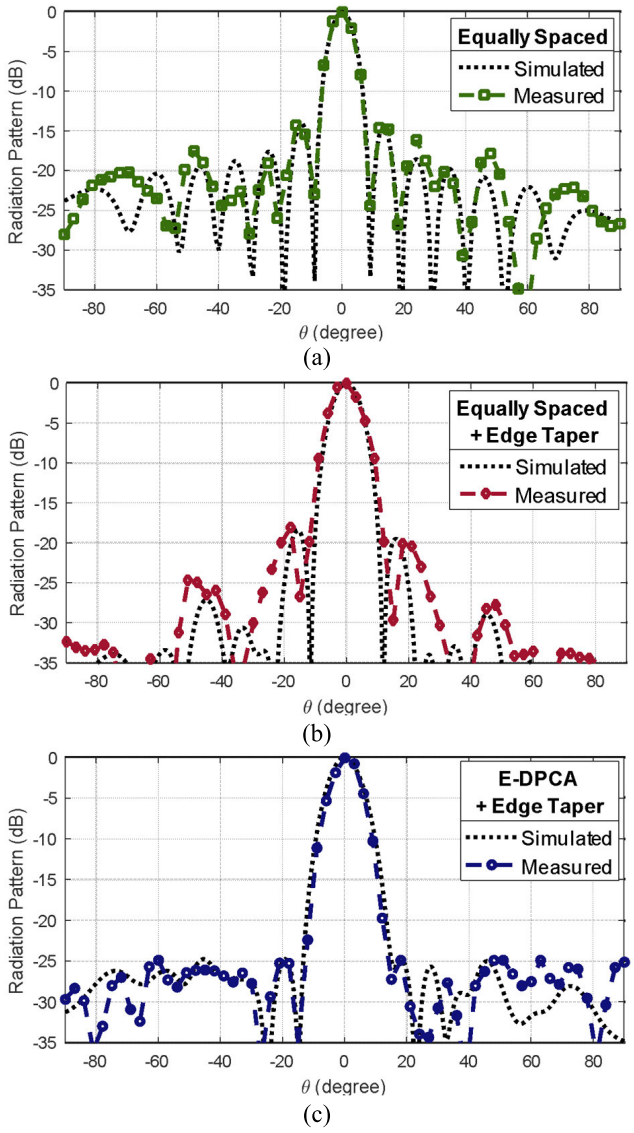

Fig. 9. Normalized radiation patterns for the nine-element linear array in the cases with (a) equally spaced (b) equally spaced with four-element edge taper, and (c) E-DPCA with four-element edge taper.

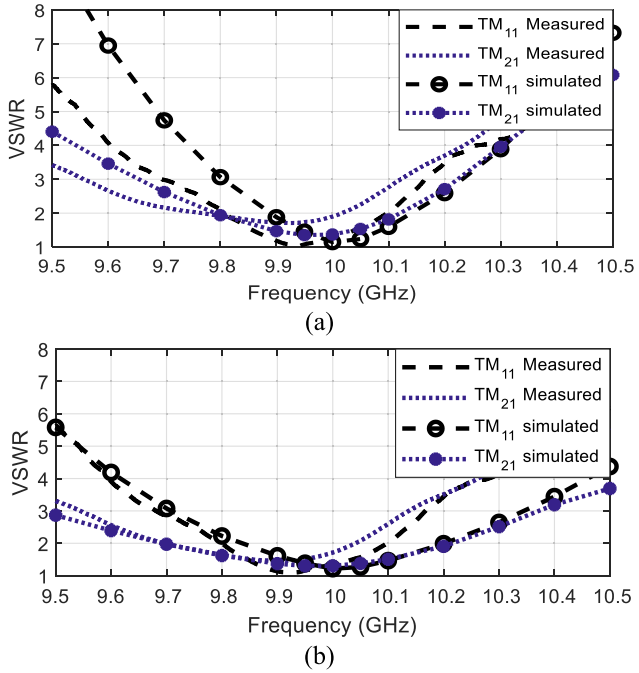

Fig. 10. Simulated and measured passive VSWR for (a) center elements and (b) edge elements in the nine-element linear array.

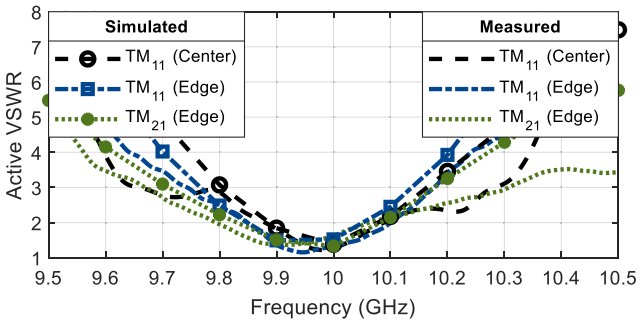

Fig. 11. Simulated and measured active VSWR in the nine-element array. For the central element, only the TM_{11} mode is excited. For the edge element, both the TM_{11} and TM_{21} modes are excited.

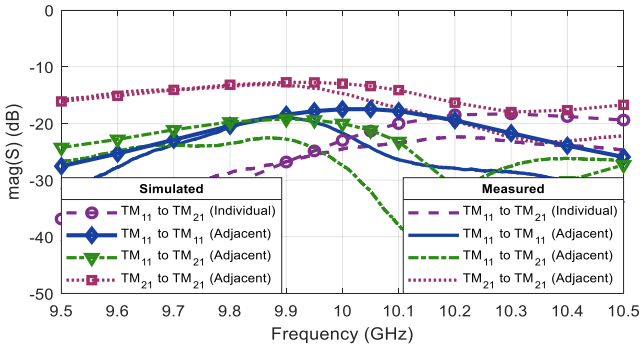

Fig. 12. Simulated and measured mutual coupling between modes within an element and between adjacent elements in the nine-element linear array.

active radiation patterns of the individual TM_{11} and TM_{21} modes were measured separately in UAH's anechoic chamber and the total radiation patterns of the array were then computed according to the excitation coefficients of the array and the mode content factors of the dual-mode base elements for the three different cases, including the uniformly excited, equally spaced array, the edge-tapered equally spaced array, and the proposed E-DPCA plus edge tapered array. The normalized radiation patterns for the three cases were measured using this setup in comparison to the full-wave simulated results. Fig. 9(a) gives the equally spaced pattern, where the SLL is quite high and close to -15 dB. Fig. 9(b) shows the equally spaced array with four edge elements tapered, in which the SLL has lowered by 3 dB. The combined effect of using edge tapering and the proposed E-DPCA technique is displayed in Fig. 9(c), where a -25 dB SLL is achieved, resulting in a 10 dB SLL reduction compared to the uniformly excited, equally spaced array. The measured results show good agreement with the simulation and combining these two approaches enables a -25 dB SLL.

The passive VSWRs of center and edge elements in this array were also measured and are presented in Fig. 10. For center elements, the measured 2:1 VSWR bandwidth (BW) is

0.3 GHz (3% fractional BW) for the TM_{11} mode and 0.2 GHz (2% fractional BW) for the TM_{21} mode. For edge elements, these BWs are 0.3 GHz (3% fractional BW) for TM_{11} and 0.32 GHz (3.2% fractional BW) for TM_{21}. The active VSWRs are plotted in Fig. 11 using only the TM_{11} mode for the center element and both modes for the edge element. This resulted in a 2:1 active VSWR BW of 0.2 GHz or 2% fractional BW, in the worst case.

Several instances of mutual coupling were also considered for this array: the mutual coupling between the TM_{11} and TM_{21} ports within one element and the mutual coupling between each port of adjacent elements. These results are summarized in Fig. 12, showing less than -10 dB of mutual coupling in the worst case.

V. Conclusion

This article has investigated the use of electronic positional control with amplitude tapering in selected elements for side and minor lobe reductions. Small linear arrays of 7-, 9-, and 11-elements were studied with varying partial amplitude control. The mode content factors and amplitude tapers were optimized for these cases. The nine-element case with four tapered edge elements was measured to validate this technique, and good agreement was found with the simulation. Edge tapering in conjunction with the E-DPCA had a significant effect on lowering the sidelobes. As an illustration of this method's effectiveness for small arrays in comparison with other methods, the results of the phase-only sidelobe suppression method from [7] on linear arrays are given in Table V. The impressive SLL characteristics of the combined E-DPCA and edge tapering technique for small arrays is then made clear.

Acknowledgment

The authors would like to thank Jonathan Marquardt for his help with the preparation of the originally submitted manuscript and Joshua Prang for his assistance in plotting the amplitude distributions and radiation patterns in MATLAB.

References

[1] C. A. Balanis, *Antenna Theory: Analysis and Design*, 4th ed. Hoboken, NJ, USA: Wiley, 2016.

[2] S. J. Stone, "Directive antenna array," U.S. Patents 1 643 323, Sep. 27, 1927.

[3] C. L. Dolph, "A current distribution for broadside arrays which optimizes the relationship between beam width and side-lobe level," *Proc. IRE*, vol. 34, no. 6, pp. 335–348, Jun. 1946.

[4] T. T. Taylor, "Design of line source antennas for narrow beamwidth and low sidelobes," *IRE Trans. Antennas Propag.*, vol. AP-3, no. 1, pp. 16–28, Jan. 1955.

[5] T. T. Taylor, "One parameter family of line-sources producing modified $\sin(\pi u)/\pi u$ patterns," Hughes Aircr. Company, Culver City, CA, USA, Tech. Memo 324, Sep. 1953.

[6] K.-K. Yan and Y. Lu, "Sidelobe reduction in array-pattern synthesis using genetic algorithm," *IEEE Trans. Antennas Propag.*, vol. 45, no. 7, pp. 1117–1122, Jul. 1997.

[7] J. F. DeFord and O. P. Gandhi, "Phase-only synthesis of minimum peak sidelobe patterns for linear and planar arrays," *IEEE Trans. Antennas Propag.*, vol. 36, no. 2, pp. 191–201, Feb. 1988.

[8] J. F. DeFord and O. P. Gandhi, "Mutual coupling and sidelobe tapers in phase-only antenna synthesis for linear and planar arrays," *IEEE Trans. Antennas Propag.*, vol. 36, no. 11, pp. 1624–1629, Nov. 1988.

[9] T. B. Vu, "Method of null steering without using phase shifters," *IEE Proc. H, Microw., Opt. Antennas*, vol. 131, pp. 242–246, Aug. 1984.

[10] H. Steyskal, R. Shore, and R. Haupt, "Methods for null control and their effects on the radiation pattern," *IEEE Trans. Antennas Propag.*, vol. AP-34, no. 3, pp. 404–409, Mar. 1986.

[11] S. Applebaum, "Adaptive arrays," *IEEE Trans. Antennas Propag.*, vol. AP-24, no. 5, pp. 585–598, Sep. 1976.

[12] R. Haupt, "Null synthesis with phase and amplitude controls at the subarray outputs," *IEEE Trans. Antennas Propag.*, vol. AP-33, no. 5, pp. 505–509, May 1985.

[13] J. A. Hejres, "Null steering in phased arrays by controlling the positions of selected elements," *IEEE Trans. Antennas Propag.*, vol. 52, no. 11, pp. 2891–2895, Nov. 2004.

[14] H. M. Elkamchouchi and M. M. Hassan, "Array pattern synthesis approach using a genetic algorithm," *IET Microw., Antennas Propag.*, vol. 8, no. 14, pp. 1236–1240, Nov. 2014.

[15] R. Elliott and G. Stern, "A new technique for shaped beam synthesis of equispaced arrays," *IEEE Trans. Antennas Propag.*, vol. AP-32, no. 10, pp. 1129–1133, Oct. 1984.

[16] R. Haupt, "Simultaneous nulling in the sum and difference patterns of a monopulse antenna," *IEEE Trans. Antennas Propag.*, vol. AP-32, no. 5, pp. 486–493, May 1984.

[17] R. Harrington, "Sidelobe reduction by nonuniform element spacing," *IRE Trans. Antennas Propag.*, vol. 9, no. 2, pp. 187–192, Mar. 1961.

[18] A. Ishimaru, "Theory of unequally-spaced arrays," *IRE Trans. Antennas Propag.*, vol. 10, no. 6, pp. 691–702, Nov. 1962.

[19] H. Unz, "Linear arrays with arbitrarily distributed elements," *IRE Trans. Antennas Propag.*, vol. 8, no. 2, pp. 222–223, Mar. 1960.

[20] J.-H. Bae, K.-T. Kim, J.-H. Lee, H.-T. Kim, and J.-I. Choi, "Design of steerable non-uniform linear array geometry for side-lobe reduction," *Microw. Opt. Technol. Lett.*, vol. 36, no. 5, pp. 363–367, Mar. 2003.

[21] F. Hodjat and S. Hovanessian, "Nonuniformly spaced linear and planar array antennas for sidelobe reduction," *IEEE Trans. Antennas Propag.*, vol. AP-26, no. 2, pp. 198–204, Mar. 1978.

[22] T. H. Ismail and M. M. Dawoud, "Null steering in phased arrays by controlling the element positions," *IEEE Trans. Antennas Propag.*, vol. 39, no. 11, pp. 1561–1566, Nov. 1991.

[23] M. M. Dawoud and T. H. Ismail, "Experimental verification of null steering by element position perturbations," *IEEE Trans. Antennas Propag.*, vol. 40, no. 11, pp. 1431–1434, Nov. 1992.

[24] A. Ishimaru, "Unequally spaced arrays based on the Poisson sum formula," *IEEE Trans. Antennas Propag.*, vol. 62, no. 4, pp. 1549–1554, Apr. 2014.

[25] R. L. Haupt, "Partial nonuniform spacing of array elements," in *Proc. IEEE Antennas Propag. Soc. Int. Symp.*, London, ON, Canada, Jun. 1991, pp. 1708–1711.

[26] K. Tomiyasu, "Combined equal and unequal element spacings for low sidelobe pattern of a symmetrical array with equal-amplitude elements," *IEEE Trans. Antennas Propag.*, vol. 39, no. 2, pp. 265–266, Feb. 1991.

[27] R. L. Haupt, "Optimized element spacing for low sidelobe concentric ring arrays," *IEEE Trans. Antennas Propag.*, vol. 56, no. 1, pp. 266–268, Jan. 2008.

[28] M. Khalaj-Amirhosseini, G. Vecchi, and P. Pirinoli, "Near-Chebyshev pattern for nonuniformly spaced arrays using zeros matching method," *IEEE Trans. Antennas Propag.*, vol. 65, no. 10, pp. 5155–5161, Oct. 2017.

[29] M. Khalaj-Amirhosseini, "Design of nonuniformly spaced antenna arrays using Fourier's coefficients equating method," *IEEE Trans. Antennas Propag.*, vol. 66, no. 10, pp. 5326–5332, Oct. 2018.

[30] S. Chatterjee and S. Chatterjee, "Pattern synthesis of centre fed linear array using Taylor one parameter distribution and restricted search particle swarm optimization," *J. Commun. Technol. Electron.*, vol. 59, no. 11, pp. 1112–1127, Nov. 2014.

[31] D. G. Kurup, M. Himdi, and A. Rydberg, "Synthesis of uniform amplitude unequally spaced antenna arrays using the differential evolution algorithm," *IEEE Trans. Antennas Propag.*, vol. 51, no. 9, pp. 2210–2217, Sep. 2003.

[32] C. Lin, A. Qing, and Q. Feng, "Synthesis of unequally spaced antenna arrays by using differential evolution," *IEEE Trans. Antennas Propag.*, vol. 58, no. 8, pp. 2553–2561, Aug. 2010.

[33] R. Wang, Y. Jiao, H. Zhang, and Z. Zhou, "Synthesis of unequally spaced linear arrays using modified differential evolution algorithm," *IET Microw., Antennas Propag.*, vol. 12, no. 12, pp. 1908–1912, Oct. 2018.
[34] F. Tokan and F. Güneş, "Interference suppression by optimising the positions of selected elements using generalised pattern search algorithm," *IET Microw., Antennas Propag.*, vol. 5, no. 2, pp. 127–135, Jan. 2011.
[35] H. Oraizi and M. Fallahpour, "Nonuniformly spaced linear array design for the specified beamwidth/sidelobe level or specified directivity/sidelobe level with coupling consideration," *Prog. Electromagn. Res. M*, vol. 4, pp. 185–209, 2008.
[36] C.-C. Yu, "Sidelobe reduction of asymmetric linear array by spacing perturbation," *Electron. Lett.*, vol. 33, no. 9, pp. 730–732, Apr. 1997.
[37] B. Q. You, L. R. Cai, J. H. Zhou, and H. T. Chou, "Hybrid approach for the synthesis of unequally spaced array antennas with sidelobes reduction," *IEEE Antennas Wireless Propag. Lett.*, vol. 14, pp. 1569–1572, 2015.
[38] K. Guney and M. Onay, "Amplitude-only pattern nulling of linear antenna arrays with the use of bees algorithm," *Prog. Electromagn. Res.*, vol. 70, pp. 21–36, 2007.
[39] M. A.-A. Mangoud and H. M. Elragal, "Antenna array pattern synthesis and wide null control using enhanced particle swarm optimization," *Prog. Electromagn. Res. B*, vol. 17, pp. 1–14, 2009.
[40] A. Tennant, M. M. Dawoud, and A. P. Anderson, "Array pattern nulling by element position perturbations using a genetic algorithm," *Electron. Lett.*, vol. 30, no. 3, pp. 174–176, Feb. 1994.
[41] T. H. Ismail and Z. M. Hamici, "Array pattern synthesis using digital phase control by quantized particle swarm optimization," *IEEE Trans. Antennas Propag.*, vol. 58, no. 6, pp. 2142–2145, Jun. 2010.
[42] M. M. Khodier and C. G. Christodoulou, "Linear array geometry synthesis with minimum sidelobe level and null control using particle swarm optimization," *IEEE Trans. Antennas Propag.*, vol. 53, no. 8, pp. 2674–2679, Aug. 2005.
[43] S. K. Goudos, V. Moysiadou, T. Samaras, K. Siakavara, and J. N. Sahalos, "Application of a comprehensive learning particle swarm optimizer to unequally spaced linear array synthesis with sidelobe level suppression and null control," *IEEE Antennas Wireless Propag. Lett.*, vol. 9, pp. 125–129, 2010.
[44] Z. A. Pour, "Control of phase center and polarization in circular microstrip antennas," M.S. thesis, Dept. Elect. Eng., Univ. Manitoba, Winnipeg, MB, Canada, Jul. 2006.
[45] T. Mitha and M. Pour, "Principles of adaptive element spacing in linear array antennas," *Sci. Rep.*, vol. 11, no. 1, p. 5584, Mar. 2021.
[46] T. H. Mitha and M. Pour, "Sidelobe reductions in linear array antennas using electronically displaced phase center antenna technique," *IEEE Trans. Antennas Propag.*, vol. 70, no. 6, pp. 4369–4378, Jun. 2022.
[47] T. H. Mitha, J. Marquardt, and M. Pour, "E-DPCA synthesis technique in small linear array antennas with tapered edge elements," in *Proc. IEEE Int. Symp. Phased Array Syst. Technol. (PAST)*, Waltham, MA, USA, Oct. 2022, pp. 1–2, doi: 10.1109/PAST49659.2022.9974990.
[48] Z. Iqbal, T. Mitha, and M. Pour, "A self-nulling single-layer dual-mode microstrip patch antenna for grating lobe reduction," *IEEE Antennas Wireless Propag. Lett.*, vol. 19, no. 9, pp. 1506–1510, Sep. 2020.
[49] D. M. Pozar, "The active element pattern," *IEEE Trans. Antennas Propag.*, vol. 42, no. 8, pp. 1176–1178, Aug. 1994.
[50] D. F. Kelley and W. L. Stutzman, "Array antenna pattern modeling methods that include mutual coupling effects," *IEEE Trans. Antennas Propag.*, vol. 41, no. 12, pp. 1625–1632, Dec. 1993.

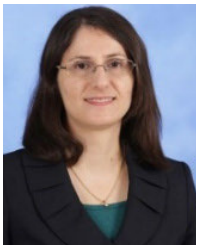

Maria Pour (Senior Member, IEEE) received the Ph.D. degree in electrical engineering from the University of Manitoba, Winnipeg, MB, Canada, in 2012.

She is an Associate Professor with the Department of Electrical and Computer Engineering, The University of Alabama in Huntsville, AL, USA. She has coauthored six book chapters and has published over 100 journal articles and conference proceedings. Her research interests are in the areas of applied electromagnetics and antennas, including phased array antennas, multimode antennas, wideband reconfigurable antennas, virtual aperture antennas, reflector antennas and feeds, primary matched feeds, and antenna measurement techniques.

Dr. Pour received the 2017 CAREER Award from the U.S. National Science Foundation. She was named the 2017 Outstanding Junior Faculty and the 2017 Outstanding Research Faculty by the College of Engineering, The University of Alabama in Huntsville. She was the recipient of the 2020 Outstanding Teaching Award of the College of Engineering and the 2021 Joseph Dowdle Outstanding Faculty Award of the Department of Electrical and Computer Engineering, The University of Alabama in Huntsville. She has been serving as a Track Editor for the IEEE TRANSACTIONS ON ANTENNAS AND PROPAGATION and as an Associate Editor for the IEEE ANTENNAS AND WIRELESS PROPAGATION LETTERS, since 2022 and 2020, respectively. She also served as an Associate Editor for the IEEE TRANSACTIONS ON ANTENNAS AND PROPAGATION from 2016 to 2022.

Tanzeela H. Mitha (Member, IEEE) was born in Pune, India, in 1993. She received the B.E. degree in electronics and telecommunication from the University of Pune, Pune, in 2016, and the Ph.D. degree in electrical engineering from The University of Alabama in Huntsville, Huntsville, AL, USA, in 2022.

She is currently a Research and Development Specialist at Avery Dennison, Azusa, CA, USA. Her research interests include microstrip patch antennas, wideband antennas, radio frequency identification (RFID) tag antennas, and phased array antennas.

Eli C. Brothers (Student Member, IEEE) was raised in Susan Moore, AL, USA. He received the B.S.E.E. degree from the University of Alabama in Huntsville, Huntsville, AL, in 2023, where he is currently pursuing the M.S.E.E. degree.

He is currently working as a Junior Electrical Engineer at Aviation & Missile Solutions, Huntsville, performing research and solutions integration in the fields of communications, radar, and antennas. His research interests include phased array antennas, reconfigurable antennas, and sparse array design in radars.